

# THE COSMIC EVOLUTION OF MASSIVE BLACK HOLES AND GALAXY SPHEROIDS: GLOBAL CONSTRAINTS AT REDSHIFT $Z \lesssim 1.2$

XIAOXIA ZHANG<sup>1</sup>, YOUJUN LU<sup>1</sup> & QINGJUAN YU<sup>2</sup>

<sup>1</sup> National Astronomical Observatories, Chinese Academy of Sciences, Beijing, 100012, China; luyj@nao.cas.cn

<sup>2</sup> Kavli Institute for Astronomy and Astrophysics, Peking University, Beijing, 100871, China; yuqj@pku.edu.cn

*Draft version May 25, 2018*

## ABSTRACT

We study the observational constraints on the cosmic evolution of the relationships between the massive black hole (MBH) mass ( $M_{\bullet}$ ) and the stellar mass ( $M_{*,\text{sph}}$ ; or velocity dispersion  $\sigma$ ) of the host galaxy/spheroid. Assuming that the  $M_{\bullet} - M_{*,\text{sph}}$  (or  $M_{\bullet} - \sigma$ ) relation evolves with redshift as  $\propto (1+z)^{\Gamma}$ , the MBH mass density can be obtained from either the observationally determined galaxy stellar mass functions or velocity dispersion distribution functions over redshift  $z \sim 0 - 1.2$  for any given  $\Gamma$ . The MBH mass density at different redshifts can also be inferred from the luminosity function of QSOs/AGNs provided known radiative efficiency  $\epsilon$ . By matching the MBH density inferred from galaxies to that obtained from QSOs/AGNs, we find that  $\Gamma = 0.64_{-0.29}^{+0.27}$  for the  $M_{\bullet} - M_{*,\text{sph}}$  relation and  $\Gamma = -0.21_{-0.33}^{+0.28}$  for the  $M_{\bullet} - \sigma$  relation, and  $\epsilon = 0.11_{-0.03}^{+0.04}$ . Our results suggest that the MBH mass growth precedes the bulge mass growth but the galaxy velocity dispersion does not increase with the mass growth of the bulge after the quench of nuclear activity, which is roughly consistent with the two-phase galaxy formation scenario proposed by Oser et al. (2012) in which a galaxy roughly double its masses after  $z = 1$  due to accretion and minor mergers while its velocity dispersion drops slightly.

*Subject headings:* black hole physics — galaxies: active — galaxies: evolution — quasars: general

## 1. INTRODUCTION

The masses of the massive black holes (MBH;  $M_{\bullet}$ ) are tightly correlated with the properties of the spheroidal components of their host galaxies, such as the velocity dispersion  $\sigma$  (e.g., Gültekin et al. 2009; Gebhardt et al. 2000; Ferrarese & Merritt 2000; Tremaine et al. 2002; Graham et al. 2011), the luminosity  $L_{\text{sph}}$  (e.g., Kormendy & Richstone 1995; McLure & Dunlop 2001), and the stellar mass  $M_{*,\text{sph}}$  (Magorrian et al. 1998; McLure & Dunlop 2002; Marconi & Hunt 2003; Häring & Rix 2004), which suggests a strong link between the growth of MBHs and the evolution of their host galaxies (or particularly the galaxy spheroids). Feedback from the nuclear activities is proposed to be responsible for the establishment of these relationships, either through momentum or energy driven winds to self-regulate the MBH growth (e.g., Silk & Rees 1998; Fabian 1999; King 2003; Wyithe & Loeb 2003; Murray et al. 2005; di Matteo et al. 2005; Croton et al. 2006; Bower et al. 2006; Somerville et al. 2008). However, the detailed physics on how the feedback mechanism processes is still not clear.

Observational determination of the cosmic evolution of the relations between  $M_{\bullet}$  and  $M_{*,\text{sph}}$  (or  $\sigma$  or  $L_{\text{sph}}$ ) may reveal important clues to the origin of these relations and put constraints on feedback mechanisms (Shields et al. 2003; Peng et al. 2006; Woo et al. 2006; Treu et al. 2007; Salviander et al. 2007; Woo et al. 2008; Alexander et al. 2008; Somerville 2009; Kisaka & Kojima 2010; Merloni et al. 2010; Sarria et al. 2010; Bennert et al. 2010, 2011; Cisternas et al. 2011; Schulze & Wisotzki 2011; Portinari et al. 2012; Li et al. 2012). A number of studies have shown that the  $M_{\bullet} - M_{*,\text{sph}}$  relation in active galactic nuclei (AGNs)

evolves with redshift (or cosmic time),  $\propto (1+z)^{\Gamma}$ , where  $\Gamma \sim 0.68 - 2.1$  (e.g., Merloni et al. 2010; Bennert et al. 2011). There are also tentative observational evidences suggesting that the  $M_{\bullet} - \sigma$  relation may also evolve with redshift (e.g., Woo et al. 2006, 2008). In most of those studies, the MBH masses are derived by adopting the virial mass estimators, which are based on the mass estimates of several dozen MBHs in nearby AGNs through the reverberation mapping technique and a calibration of those masses to the  $M_{\bullet} - \sigma$  relation obtained for nearby normal galaxies (e.g., Onken et al. 2004; Graham et al. 2011). However, the MBH mass estimated from the virial mass estimators may suffer from some systematic biases due to various reasons (e.g., Krolik 2001; Collin et al. 2006; Netzer & Marziani 2010; Kollatschny & Zetzl 2011; Graham et al. 2011); moreover, the MBHs in AGNs are still growing rapidly, unlike those in nearby quiescent galaxies. Therefore, it is not yet clear whether the cosmic evolution of the  $M_{\bullet} - M_{*,\text{sph}}$  relation and the  $M_{\bullet} - \sigma$  relation found for AGNs are biased or not and whether the relations for normal galaxies has a similar cosmic evolution as those for AGNs.

In this paper, we adopt an alternative way to investigate the cosmic evolution of the  $M_{\bullet} - M_{*,\text{sph}}$  relation and the  $M_{\bullet} - \sigma$  relation in normal galaxies by matching the MBH mass density inferred from normal galaxies at different redshifts with that inferred from AGNs. The evolution of the  $M_{\bullet} - M_{*,\text{sph}}$  and  $M_{\bullet} - \sigma$  relations for normal galaxies is assumed to follow a simple power-law form, i.e.,  $\propto (1+z)^{\Gamma}$ . In Section 2, we estimate the evolution of the MBH mass density in normal galaxies by the two ways: (i) using the stellar mass functions (SMFs) of galaxies determined by recent observations over the redshift range  $z \sim 0 - 1.2$  (e.g., Bernardi et al. 2010; Ilbert et al. 2010), and (ii) using the velocity dis-

persion functions (VDFs) of galaxies at  $z \sim 0 - 1.5$  (Bernardi et al. 2010; Bezanson et al. 2011). The evolution of the estimated MBH densities depends on the parameter  $\Gamma$ . According to the simple Softan (1982) argument, the MBH mass density evolution can also be derived from the AGN luminosity functions (LFs), as shown in Section 2.3, where the parameter  $\Gamma$  is not involved. By matching the MBH density evolution inferred from properties of normal galaxies to that inferred from AGNs, the cosmic evolution of the  $M_\bullet - M_{*,\text{sph}}$  (or  $M_\bullet - \sigma$ ) relation is then constrained in Section 3. Discussion and conclusions are given in Sections 4 and 5.

Throughout the paper, we adopt the cosmological parameters  $H_0 = 70.5 \text{ km s}^{-1}$ ,  $\Omega_\Lambda = 0.726$ , and  $\Omega_M = 0.274$  (Komatsu et al. 2009). The mass is in units of  $M_\odot$  and the velocity dispersion is in units of  $\text{km s}^{-1}$ . Given a physical variable  $X$  (e.g., mass, logarithm of mass, velocity distribution), the  $X$  function is denoted by  $n_X(X, z)$  so that  $n_X(X, z)dX$  represents the comoving number density of the objects (e.g., MBHs or galaxies) with variable  $X$  in the range  $X \rightarrow X + dX$  at redshift  $z$ .

## 2. THE MASS DENSITY EVOLUTION OF MASSIVE BLACK HOLES

### 2.1. The mass density of massive black holes inferred from stellar mass functions

The mass of a MBH in the center of a nearby ( $z \sim 0$ ) normal galaxy can be estimated through the  $M_\bullet - M_{*,\text{sph}}$  relation at  $z = 0$ , i.e.,

$$\langle \log M_\bullet \rangle (M_{*,\text{sph}}; z = 0) = (8.20 \pm 0.10) + (1.12 \pm 0.06) \times (\log M_{*,\text{sph}} - 11), \quad (1)$$

where  $\langle \log M_\bullet \rangle (M_{*,\text{sph}}; z = 0)$  is the mean value of the logarithmic MBH masses for galaxies with spheroidal mass  $M_{*,\text{sph}}$ , and the intrinsic scatter of  $\log M_\bullet(M_{*,\text{sph}}; z = 0)$  around this mean value is 0.3 dex (Häring & Rix 2004, see also McLure & Dunlop 2002). Currently, there is still no consensus on the  $M_\bullet - M_{*,\text{sph}}$  relation for galaxies at high redshift. In general, the  $M_\bullet - M_{*,\text{sph}}$  relation may evolve with redshift and the evolution may be simplified by

$$\langle \log M_\bullet \rangle (M_{*,\text{sph}}; z) = \langle \log M_\bullet \rangle (M_{*,\text{sph}}; z = 0) + \Gamma \log(1 + z) \quad (2)$$

as assumed in a number of previous works (e.g., Merloni et al. 2010; Bennert et al. 2011), where the parameter  $\Gamma$  describes the significance of the evolution, and the intrinsic scatter of the relations is assumed not to evolve with redshift.

The mass function of MBHs (BHMF) at redshift  $z$  may be estimated by adopting the  $M_\bullet - M_{*,\text{sph}}$  relation (eq. 2) and the SMF of spheroids at that redshift if the SMF can be observationally determined, i.e.,

$$n_{\log M_\bullet}(\log M_\bullet, z) = \int n_{\log M_{*,\text{sph}}}(\log M_{*,\text{sph}}, z) \times P(\log M_\bullet; \langle \log M_\bullet \rangle) d \log M_{*,\text{sph}} \quad (3)$$

where  $n_{\log M_{*,\text{sph}}}(\log M_{*,\text{sph}}, z)$  is the SMF of spheroids at redshift  $z$ ,  $P$  is the probability density function of  $\log M_\bullet$  around  $\langle \log M_\bullet \rangle$  and is assumed to be normally distributed with a dispersion of 0.3 dex. The SMF of spheroids at redshift  $z$  can be estimated by using the

SMFs for galaxies with different morphological types and the bulge-to-total mass ratios  $B/T$ , i.e.,

$$n_{\log M_{*,\text{sph}}}(\log M_{*,\text{sph}}, z) = \sum_i n_{\log M_{*,\text{sph}}}^i(\log M_{*,\text{sph}}, z) = \sum_i f^i(M_{*,\text{tot}}, z) n_{\log M_{*,\text{tot}}}(\log M_{*,\text{tot}}, z) \frac{d \log M_{*,\text{tot}}}{d \log M_{*,\text{sph}}}, \quad (4)$$

where  $M_{*,\text{tot}} = M_{*,\text{sph}}/(B/T)$ ,  $n_{\log M_{*,\text{tot}}}(\log M_{*,\text{tot}}, z)$  is the SMF for all galaxies,  $n_{\log M_{*,\text{sph}}}^i(\log M_{*,\text{sph}}, z)$  is the SMF for the spheroids of those galaxies with Hubble type  $i$ ,  $f^i(M_{*,\text{tot}}, z)$  is the fraction of galaxies with Hubble type  $i$  to all galaxies, and the summation is over galaxy morphological types from E, S0, Sa-Sb, Sc-Sd to Irr.

The SMFs for galaxies at  $z \sim 0$  with different morphological types have been obtained from the Sloan Digital Sky Survey (SDSS; Bernardi et al. 2010, see Table B2 therein). And the bulge-to-total mass ratio  $B/T$  has been given by Weinzirl et al. (2009, see Table 1) for more than a hundred nearby galaxies with different Hubble types. In summary, the bulge-to-total mass ratios are  $1, 0.28 \pm 0.02, 0.46 \pm 0.05, 0.35 \pm 0.10, 0.22 \pm 0.08, 0.15 \pm 0.05$ , and 0 for E, S0, Sa, Sab, Sb, Sc-Sd, and Irr, respectively.<sup>1</sup> Adopting these observations, the SMF of spheroids and the BHMF at  $z = 0$  can be estimated.

For galaxies at redshift  $z \sim 0.2 - 1.2$ , the total SMFs have been obtained by Ilbert et al. (2010), Pérez-González et al. (2008), Fontana et al. (2006), and Borch et al. (2006). These SMFs are usually obtained from deep surveys with small sky coverage and may suffer the cosmic variance. To avoid the cosmic variance, we adopt the average total SMFs according to the SMFs estimated in the above papers. In Ilbert et al. (2010), the SMFs of quiescent early type galaxies (E+S0) at different redshifts are directly obtained (see Table 2 therein); and we obtain the SMFs of all the galaxies by summing the SMFs of early type galaxies and those of “intermediate activity” and “high activity” galaxies (see the definition of “intermediate activity” and “high activity” in Ilbert et al. 2010, and see their Table 3). We assume that the fraction of the early-type galaxies at any given mass is the same as that given by Ilbert et al. (2010) and hereafter adopt this fraction, together with the average total SMFs, to calculate the MBH mass function for early-type galaxies. The LFs of galaxies were estimated by Zucca et al. (2006) for four different spectral types, which roughly correspond to the morphological types of E/S0, Sa-Sb, Sc-Sd, and Irr, respectively. For each type of galaxies, the mass-to-light ratio can be estimated through their average colors, for instance,  $\log(M_{*,\text{tot}}/L_B) = -0.942 + 1.737(B - V) + 0.15$  for early-type galaxies by adopting the Salpeter initial mass function and  $\log(M_{*,\text{tot}}/L_B) = -0.942 + 1.737(B - V) - 0.10$  for late-type galaxies by adopting the Chabrier initial

<sup>1</sup> Graham & Worley (2008) obtain the ratio of K-band bulge luminosity/flux to disk luminosity/flux for a large number of disk galaxies in which the dust extinction is considered and corrected. Assuming a constant mass-to-light ratio, we also alternatively adopt the  $B/D$  ratios inferred from Graham & Worley (2008) in our analysis, i.e.,  $\log(B/D) = -0.54, -0.34, -0.54, -0.6$ , and  $-1.2$  for S0, Sa, Sab, Sb, and Scd, respectively, and obtain the constraints  $(\Gamma, \epsilon) = (0.68 \pm 0.24, 0.10 \pm 0.01)$ , which is consistent with that obtained by adopting the  $B/D$  ratios given by Weinzirl et al. (2009).

mass function (Bell & De Jong 2001; Bell et al. 2003; Bernardi et al. 2010; Chabrier 2003). The  $B - V$  colors for different morphological types of galaxies are given by Fukugita et al. (1995). The luminosity evolution can be corrected for each type of galaxies according to Bell et al. (2003). The LF for galaxies with different morphological types (Zucca et al. 2006) can thus be converted to the SMFs. According to these SMFs, the relative abundance of different late-type galaxies (Sa-Sb, Sc-Sd, and Irr) over  $z \sim 0.2 - 1.2$  can be obtained at any given  $M_{*,\text{tot}}$ . The SMF of spheroids and the BHMF can then be estimated if the  $B/T$  is averagely the same for galaxies with the same spectral type (and maybe correspondingly the same morphological type) but at different redshifts. Consequently, the mass density accreted onto MBHs with mass  $> M_\bullet$  can be obtained by

$$\rho_\bullet^{\text{gal}}(z; > M_\bullet) = \int_{M_\bullet}^{\infty} (M'_\bullet - M_\bullet) n_{\log M'_\bullet}(\log M'_\bullet, z) d \log M'_\bullet, \quad (5)$$

if mergers of MBHs do not significantly contribute to the MBH growth and the seeds of those MBHs are smaller than  $M_\bullet$  [see Eq. (29) in Yu & Lu (2004) and Eq. (35) in Yu & Tremaine (2002)]. And this mass density can be directly matched by that inferred from QSOs/AGNs (see Section 2.3). Hereafter, we set the lower limit of the MBH mass in the above integration to be  $10^6 M_\odot$  unless otherwise stated, as the smallest mass for those nearby MBHs, of which the mass is well measured and adopted to determine the  $M_\bullet - M_{*,\text{sph}}$  (or  $M_\bullet - \sigma$ ) relation, is  $\sim 10^6 M_\odot$ . Given observationally well determined SMFs (or VDFs below), the MBH mass density estimated from the normal galaxies depends on the evolution parameter  $\Gamma$  in the  $M_\bullet - M_{*,\text{sph}}$  (or  $M_\bullet - \sigma$ ) relation.

### 2.2. The mass density of massive black holes inferred from velocity dispersion distribution functions

The mass of a MBH can also be estimated through the  $M_\bullet - \sigma$  relation at redshift  $z = 0$ , i.e.,

$$\langle \log M_\bullet \rangle (\sigma; z = 0) = (8.12 \pm 0.08) + (4.24 \pm 0.41) \times (\log \sigma - 2.30), \quad (6)$$

with an intrinsic scatter of 0.44 dex (Gültekin et al. 2009). Assuming an evolutionary form similar to equation (2), i.e.,

$$\langle \log M_\bullet \rangle (\sigma; z) = \langle \log M_\bullet \rangle (\sigma; z = 0) + \Gamma \log(1 + z), \quad (7)$$

the BHMF at redshift  $z$  can be estimated through

$$n_{\log M_\bullet}(\log M_\bullet, z) = \int n_\sigma^{\text{gal}}(\sigma, z) P(\log M_\bullet; \langle \log M_\bullet \rangle) d\sigma, \quad (8)$$

where  $n_\sigma^{\text{gal}}(\sigma, z)$  is the galaxy VDF at redshift  $z$ ,  $P$  is the probability density function of  $\log M_\bullet$  around  $\langle \log M_\bullet \rangle (\sigma; z)$  and is assumed to be normally distributed with a dispersion of 0.44 dex. The VDF for local galaxies has been estimated from SDSS (Bernardi et al. 2010, see Table B4 therein). At higher redshift  $z \sim 0.3 - 1.5$ , the VDFs have been obtained from UKIDSS (United Kingdom Infrared Telescope Infrared Deep Sky Survey) Ultra-Deep Survey (UDS) and NEWFIRM (NOAO Extremely Wide-Field Infrared Imager) Medium Band Sur-

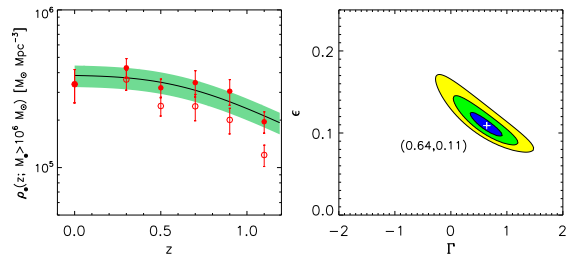


FIG. 1.— The cosmic evolution of the comoving MBH mass density. In the left panel, the red solid circles with errorbars represent the mass densities for those MBHs with mass  $> 10^6 M_\odot$ , estimated from the SMFs of normal galaxies by assuming an evolution with  $\Gamma = 0.64$  in the  $M_\bullet - M_{*,\text{sph}}$  relation (see eq. 2), which are best matched by the solid line, while the red open circles represent the mass densities estimated by assuming a universal  $M_\bullet - M_{*,\text{sph}}$  relation without evolution (i.e.,  $\Gamma = 0$ ). The solid line and the green shaded region represent the MBH mass density inferred from the hard X-ray AGN LF by assuming  $\epsilon = 0.11$  and its  $1\sigma$  uncertainty. The right panel shows the best-fit parameter  $(\Gamma, \epsilon)$  (denoted by crosses) and the contours of the confidence levels for them, obtained by matching the MBH densities inferred from the normal galaxies to that inferred from AGNs. The contours enclose the 68.3%, 95.4%, and 99.7% confidence regions on the joint distribution of the two parameters.

vey (NMBS) (Bezanson et al. 2011). Adopting those VDFs, the BHMF and consequently the mass density accreted onto MBHs with mass larger than  $M_\bullet$  can also be estimated (see Eq. 5).

### 2.3. The mass density of massive black holes inferred from AGNs

The MBH mass density at redshift  $z$  can also be inferred from the LF of AGNs according to the simple Soltan (1982) argument as MBHs obtained their mass mainly through gas accretion (e.g., Salucci et al. 1999; Yu & Tremaine 2002; Marconi et al. 2004; Yu & Lu 2004, 2008; Shankar et al. 2004, 2009), i.e.,

$$\rho_\bullet^{\text{AGN}}(z; > M_\bullet) \simeq \int_z^\infty dz \int dL_Y \int dC_Y \frac{1 - \epsilon}{\epsilon c^2} \times C_Y P(C_Y | L_Y) L_Y \phi(L_Y, z) \left| \frac{dt}{dz} \right|, \quad (9)$$

where  $L_Y$  is the AGN  $Y$ -band luminosity,  $\phi(L_Y, z)$  is the AGN  $Y$ -band luminosity function,  $\epsilon$  is the mass-to-energy conversion efficiency, and  $C_Y \equiv L_{\text{bol}}/L_Y$  is the bolometric correction (BC) for the  $Y$  band,  $L_{\text{bol}}$  is the AGN bolometric luminosity, and  $P(C_Y | L_Y) dC_Y$  gives the probability of a BC to be in a range  $C_Y \rightarrow C_Y + dC_Y$  given a  $L_Y$ . The hard X-ray LF of AGNs is adopted here because a significant number of obscured AGNs can be detected only in the hard X-ray band while missed in the optical surveys. Using the hard X-ray AGN LF and the corresponding BC, the MBH mass density can be estimated given a constant  $\epsilon$ .

The hard X-ray AGN LF has been estimated by a number of authors based on the surveys by ASCA, Chandra, and XMM in the past decade (e.g., Ueda et al. 2003; La Franca et al. 2005; Silverman et al. 2008; Ebrero et al. 2009; Yencho et al. 2009; Aird et al. 2010). In this paper, we adopt the latest 2-10 keV X-ray AGN LF obtained by Aird et al. (2010, the LADE model in their Table 4) over the redshift range  $0 \leq z \leq 3.5$  and

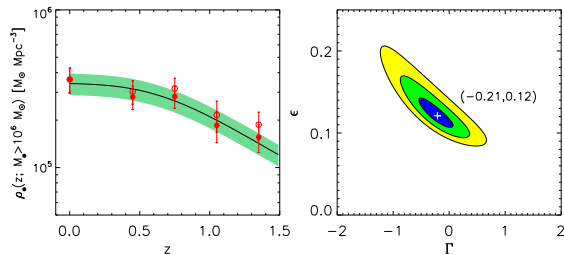


FIG. 2.— Legends are the same as those in Figure 1, except that the red solid (or red open) circles with errorbars are estimated from the VDFs of normal galaxies and by assuming an evolution with  $\Gamma = -0.21$  (or no evolution with  $\Gamma = 0$ ) in the  $M_\bullet - \sigma$  relation, and the red solid circles are best matched by the solid line estimated from the AGN LF by assuming  $\epsilon = 0.12$ .

extrapolate it to higher redshift.<sup>2</sup> Adopting other versions of the 2-10 keV AGN LF has little effects on the results presented in the following section. The BCs at the hard X-ray band (2-10 keV, denoted as  $C_X$ ) have been found to be luminosity dependent and the BC at any given bolometric luminosity has already been derived by Marconi et al. (2004) and Hopkins et al. (2007). To obtain the MBH mass density from the AGN LF, we need to estimate the probability distribution function of  $P(C_Y|L_Y)$ . Hopkins et al. (2007) obtained the probability distribution function of  $C_Y$  as a function of  $L_{\text{bol}}$ . By adopting the same procedures as those done in Hopkins et al. (2007), we fit the BCs by a log-normal distribution with the following parameters<sup>3</sup>,

$$\langle \log C_X \rangle = \log \left[ c_1 \left( \frac{L_X}{10^{10} L_\odot} \right)^{k_1} + c_2 \left( \frac{L_X}{10^{10} L_\odot} \right)^{k_2} \right], \quad (10)$$

with  $(c_1, k_1, c_2, k_2) = (26.75, 0.38, 7.44, 0.01)$ , and the scatter  $\sigma_{\log C_X} = \sigma_1 \left( \frac{L_X}{10^9 L_\odot} \right)^\beta + \sigma_2$  with  $(\sigma_1, \beta, \sigma_2) = (0.24, 0.06, -0.01)$ . Similar to Yu & Lu (2008), we then add a scatter of 0.15 dex to include the X-ray variabilities in AGNs according to Vasudevan & Fabian (2007). We adopt this fitting formula of  $C_X$  in the calculations of the MBH mass density. In the calculations of the MBH mass density from AGNs for MBHs with mass larger than  $M_\bullet$ , a lower limit is needed to set to the luminosity.

<sup>2</sup> Since the Compton-thick AGNs are not included in the hard X-ray AGN LF, which may be a fraction of  $\sim 20\%$  of the total AGN population (Malizia et al. 2009), the MBH mass densities inferred from the AGN LFs above may be underestimated by 20% and thus  $\epsilon$  for the best match is underestimated by a factor of  $\sim 1.2$ .

<sup>3</sup> We adopt the QSO spectral energy distribution (SED) model constructed by Hopkins et al. (2007). For details, the template SED consists of a power law in optical-UV band, i.e.,  $L_\nu \propto \nu^\alpha$  where  $L_\nu$  is the energy radiated per unit time per unit frequency at frequency  $\nu$ , with  $\alpha = -0.44$  for  $1\mu\text{m} < \lambda < 1300\text{\AA}$  and  $\alpha = -1.76$  from  $1200\text{\AA}$  to  $500\text{\AA}$ . At the wavelength longer than  $\lambda > 1\mu\text{m}$ , an infrared “bump” from reprocessing of optical-UV-X-ray emission is adopted and truncated as a Rayleigh-Jeans tail of the black-body emission ( $\alpha = 2$ ). The SED at energy high than 0.5 keV is determined also by a power law, with a slope of  $-0.8$ , and an exponential cut-off at 500 keV. For any given monochromatic luminosity at  $2500\text{\AA}$ , the SED is renormalized to give the optical to X-ray slope of  $\alpha_{\text{ox}} \equiv 0.384 \log(L_{\nu(2500\text{\AA})}/L_{\nu(2\text{keV})})$  and the points between 500 eV and  $500\text{\AA}$  are connected with a power law. The value of  $\alpha_{\text{ox}}$  depends on luminosity as  $\alpha_{\text{ox}} = -0.107 \log(L_{\nu(2500\text{\AA})}/\text{erg s}^{-1} \text{Hz}^{-1}) + 1.739$ . After the SED is constructed, we integrate the SED to obtain the 2–10 keV luminosity  $L_X$  and the bolometric luminosity, and hence the BCs. We fit the BCs by a double power-law function as shown in Equation (10).

As the typical Eddington ratio for low-luminosity AGNs is around 0.1 (Shen et al. 2008) or 0.2 (Graham et al. 2011). therefore, it is reasonable to set the lower limit  $L_{\text{bol}}(M_\bullet) \simeq 0.1 L_{\text{EDD}}(M_\bullet)$  or  $0.2 L_{\text{EDD}}(M_\bullet)$ . Our calculations show that the difference in the lower limit does not lead to significant difference in the results.

### 3. CONSTRAINTS ON THE COSMIC EVOLUTION OF THE $M_\bullet - M_{*,\text{sph}}$ RELATION AND THE $M_\bullet - \sigma$ RELATION

In this Section, we obtain constraints on the evolution of the  $M_\bullet - M_{*,\text{sph}}$  (or  $M_\bullet - \sigma$ ) relation by matching the MBH densities inferred from normal galaxies with that from AGNs using the standard  $\chi^2$  statistics, i.e.,

$$\chi^2 \equiv \sum_i \frac{[\rho_\bullet^{\text{gal}}(z_i, > M_\bullet) - \rho_\bullet^{\text{AGN}}(z_i, > M_\bullet)]^2}{[\delta\rho_\bullet^{\text{gal}}(z_i, M_\bullet)]^2 + [\delta\rho_\bullet^{\text{AGN}}(z_i, > M_\bullet)]^2}, \quad (11)$$

where  $z_i$  is the  $i$ -th redshift bin and the summation is over all the redshift bins,  $\delta\rho_\bullet^{\text{gal}}(z_i, > M_\bullet)$  and  $\delta\rho_\bullet^{\text{AGN}}(z_i, > M_\bullet)$  are the uncertainties in the MBH mass densities estimated from the normal galaxies and AGNs, respectively, considering the  $1\sigma$  errors in most of the fitting parameters for the SMFs/VDFs and the AGN LFs, and the  $M_\bullet - M_{*,\text{sph}}$  and  $M_\bullet - \sigma$  relations. The errors in the normalizations of the  $M_\bullet - M_{*,\text{sph}}$  and  $M_\bullet - \sigma$  relations and the AGN LF only introduce systematic shifts of all the estimates but do not lead to a change in the shape of the cosmic evolution of the MBH density, therefore, we do not include them in  $\delta\rho_\bullet^{\text{gal}}(z_i, > M_\bullet)$  and  $\delta\rho_\bullet^{\text{AGN}}(z_i, > M_\bullet)$  in the  $\chi^2$  fitting here.

Figure 1 shows the mass densities of those MBHs with mass  $> 10^6 M_\odot$  estimated from the SMFs of normal galaxies, which are best matched by the MBH densities estimated from the hard X-ray AGN LFs. The corresponding parameters for the best match are  $(\Gamma, \epsilon) = (0.64_{-0.29}^{+0.27}, 0.11_{-0.01}^{+0.02})$  and the errors are obtained for each parameter by marginalizing over the other parameter. According to our calculations, a  $\Gamma$  larger than 1.6 is excluded at the  $3\sigma$  level. The value of  $\Gamma = 0.65$  suggests that the  $M_\bullet - M_{*,\text{sph}}$  relation evolves with redshift positively, i.e., the relative positive offset of the  $M_\bullet - M_{*,\text{sph}}$  relation at redshift  $z$  to that at local universe increases with increasing redshift. Figure 2 shows the MBH mass densities estimated from the VDFs of normal galaxies, which are also best matched by the MBH densities estimated from the hard X-ray AGN LFs. The corresponding parameters for the best match are  $(\Gamma, \epsilon) = (-0.21_{-0.33}^{+0.28}, 0.12_{-0.01}^{+0.02})$ , which suggests that the  $M_\bullet - \sigma$  relation does not evolve with redshift. The  $\epsilon$  obtained by adopting the  $M_\bullet - \sigma$  relation is larger, which is because the MBH densities at  $z \sim 0$  estimated from the  $M_\bullet - \sigma$  relation is smaller than that from the  $M_\bullet - M_{*,\text{sph}}$  relation. Considering the  $1\sigma$  errors in the normalizations of the  $M_\bullet - M_{*,\text{sph}}$  and  $M_\bullet - \sigma$  relations and the AGN LF, there are the additional errors  $\pm 0.03$  in the estimated  $\epsilon$ . By combining these additional errors with the errors obtained from the above  $\chi^2$  fitting and averaging the  $\epsilon$  obtained from the two relations, we have  $\epsilon = 0.11_{-0.03}^{+0.04}$ , which is consistent with the constraint obtained in Yu & Lu (2008).

As seen from Figures 1 and 2, the MBH mass density at  $z \sim 0$  is about  $(3.5 - 4) \times 10^5 M_\odot$ , which may

be slightly smaller than that obtained by others (e.g., Graham & Driver 2007; Shankar et al. 2009). This difference is mainly due to the difference in the normalization of the adopted  $M_\bullet - \sigma$  relation and different treatment on the dependence of the MBH mass density on the Hubble constant. These differences lead to a change of the MBH density estimates at different redshifts by the same factor, but the shape of the MBH density evolution does not change and thus the constraint on  $\Gamma$  is not affected.

In the above calculations of the MBH mass densities, the SMFs and VDFs are extrapolated to the low-mass or low-velocity dispersion end, of which part may be not accurately determined by the observations at all the redshifts considered in this paper (see Ilbert et al. 2010; Bezanson et al. 2011). To see whether the final results are affected by the extrapolation, we also set the lower limit of the MBH mass to  $10^8 M_\odot$  and re-do the above matching. And we find  $(\Gamma, \epsilon) = (0.61_{-0.20}^{+0.21}, 0.18_{-0.02}^{+0.02})$  to match the MBH mass densities estimated from the SMFs of normal galaxies with that estimated from the AGNs, and find  $(\Gamma, \epsilon) = (-0.62_{-0.20}^{+0.20}, 0.19_{-0.01}^{+0.02})$  to match the MBH mass densities estimated from the VDFs of normal galaxies. The constraints on  $(\Gamma, \epsilon)$  for MBHs with mass  $> 10^8 M_\odot$  are roughly consistent with that for MBHs with mass  $> 10^6 M_\odot$ .

#### 4. DISCUSSION

The positive evolution of the  $M_\bullet - M_{*,\text{sph}}$  relation found in this paper is consistent with that found by Merloni et al. (2010) (see also Jahnke et al. 2009 and Bennert et al. 2011), which suggests that the growth of MBHs predates the assembly of spheroids and the spheroids experience additional growth after the quench of their central nuclear activities. The non-evolution of the  $M_\bullet - \sigma$  relation found here appears different from the positive evolution found by Woo et al. (2006, 2008). We note here that this difference may be lessened as the MBH masses estimated in Woo et al. (2006) and Woo et al. (2008) may be over-estimated by a factor of two as suggested by the uncertainties in the virial factor recently revealed by Graham et al. (2011). However, the exact reason for this difference is not clear as our results are obtained through the global evolution of the MBH mass densities, different from the way adopted in Woo et al. (2006, 2008) for a sample of individual AGNs/QSOs. And the VDFs estimated by Bezanson et al. (2011) are the very first estimates of VDFs at redshift  $z \neq 0$ , which may suffer from various uncertainties as discussed in Bezanson et al. (2011). If the non-evolution of the  $M_\bullet - \sigma$  relation is true, nevertheless, it suggests the velocity dispersion of galactic bulges does not increase although the masses of the bulges can be significantly enlarged after the quench of their central nuclear activities.

The evolution of the relations between the MBH mass and galaxy properties are intensively investigated theoretically in the scenario of co-evolution of galaxies and MBHs since the discovery of these scaling relations. For those early models that adopt rapid and strong feedback due to energy output from the central AGNs which terminates star formation, the scaling relations are expected to evolve little and have very small scat-

ters (e.g., Granato et al. 2004; Robertson et al. 2006; di Matteo et al. 2005; Springel et al. 2005). Later models do suggest that the  $M_\bullet - M_{*,\text{sph}}$  relation evolve positively with redshift though with various degrees of evolution (e.g., Hopkins et al. 2007; Croton et al. 2006; Fontanot et al. 2006; Malbon et al. 2007; Lamastra et al. 2010), by considering detailed dissipation processes occurred during major mergers of galaxies and the acquiring of bulge masses by dynamical processes such as disk instabilities or disrupting stellar discs. However, the expected  $M_\bullet - \sigma$  relation is almost independent of redshift (Hopkins et al. 2007). Apparently the constraints that we obtained in this paper are roughly consistent with the theoretical studies of Hopkins et al. (2007). Furthermore, we note that Oser et al. (2010, see also Oser et al. 2012) recently proposed a two-phase galaxy formation scenario, in which galaxies roughly double their masses after  $z = 1$  due to accretion and minor mergers while velocity dispersion drops slightly. If MBHs mainly obtained their masses through efficient accretion triggered by major mergers, then our constraints are consistent with the two-phase galaxy formation scenario.

#### 4.1. Mass-to-energy conversion efficiency in AGNs/QSOs

The constraints on  $\Gamma$  obtained above may depend on the use of a constant  $\epsilon$ , i.e.,  $\epsilon$  is independent of  $M_\bullet$ , redshift, and other physical quantities involved in the accretion processes. We argue that the use of a constant  $\epsilon$  in AGNs/QSOs is appropriate as follows: (1)  $\epsilon$  is determined mainly by the spins of MBHs in the standard disk accretion scenario; (2) the majority of the AGNs/QSOs are accreting via thin disks with high Eddington ratios ( $\gtrsim 0.1$ ); and (3) the spins of individual MBHs can quickly reach an equilibrium value and stay at that value for most of the AGN lifetime as suggested by theoretical models (e.g., Volonteri et al. 2005; Shapiro 2005; Hawley et al. 2007; Maio et al. 2012), which suggests a roughly constant  $\epsilon$  at all redshift. Note that some authors introduced a dependence of  $\epsilon$  on the redshift or MBH mass, such as Davis & Laor (2011); Martínez-Sansigre & Rawlings (2012); Li et al. (2012), etc., according to the current observations. However, these results may be only due to some observational biases (e.g., Raimundo et al. 2012) and need further investigation. Nevertheless, we note here that one could also introduce a cosmic evolution to  $\epsilon$  before understanding the underlying physics. For example, if we assume  $\epsilon(z) = \max\{0.057, \min[\epsilon_0(1+z)^\kappa, 0.31]\}$  but the  $M_\bullet - M_{*,\text{sph}}$  relation does not evolve with redshift, where 0.31 and 0.057 are the  $\epsilon$  that an efficiently accreting MBH-disk system could reach if the MBH spin is either 0.998 (the maximum spin of a MBH, see Thorne 1974) or 0 (a Schwarzschild MBH). In this case, an acceptable fit can also be found and the best-fit parameters are  $(\kappa, \epsilon_0) = (1.3_{-0.4}^{+0.9}, 0.04_{-0.02}^{+0.01})$  for the  $M_\bullet - M_{*,\text{sph}}$  relation, which suggests that  $\epsilon$  is significantly higher at  $z \sim 2$  than at  $z \sim 0$ . However, the MBH densities estimated from AGNs are an integration of  $\frac{d\rho_\bullet}{dz}$  over  $z$ , and  $\frac{d\rho_\bullet}{dz}$  is a function of  $\epsilon(z)$  and has to be determined to high redshift. The MBH densities estimated from the SMFs in this paper only cover the redshift up to  $\sim 1.2$  and may poorly constrain the evolution of  $\epsilon(z)$  at higher  $z$ . If  $\epsilon$  is significantly higher at higher redshift, a significantly

negative evolution in the  $M_{\bullet} - \sigma$  relation is required. Future measurements on the SMFs and VDFs at  $z \gtrsim 1.2$  may help to determine the MBH densities at higher  $z$  and thus may further help to put constraints on whether  $\epsilon$  significantly evolves with redshift.

To close the discussion on this issue, we remark here that the constraint on the cosmic evolution of the  $M_{\bullet} - M_{*,\text{sph}}$  (or  $M_{\bullet} - \sigma$ ) relation obtained in this paper is robust if the efficiency  $\epsilon$  of the efficient accretion processes in QSOs/AGNs is roughly a constant, which may be true as suggested by some physical models of the spin evolution of MBHs (e.g., Volonteri et al. 2005; Shapiro 2005; Hawley et al. 2007; Maio et al. 2012).

#### 4.2. Intrinsic scatters in the $M_{\bullet} - M_{*,\text{sph}}$ or the $M_{\bullet} - \sigma$ relation

The intrinsic scatters in the  $M_{\bullet} - M_{*,\text{sph}}$  and the  $M_{\bullet} - \sigma$  relations have been assumed not to evolve with redshift in obtaining the constraints on the cosmic evolution of the relations. If the intrinsic scatter in the  $M_{\bullet} - M_{*,\text{sph}}$  relation increases significantly with increasing redshift, the parameter  $\Gamma$  can still be consistent with 0 to match the MBH densities estimated from normal galaxies to that from AGNs. To settle onto the observed local  $M_{\bullet} - M_{*,\text{sph}}$  relation with a smaller intrinsic scatter but with the same normalization, however, it is necessary for those galaxies at a fixed  $M_{*,\text{sph}}$  with relative large MBHs to accrete more stars and for those with relatively small MBHs not to accrete many stars after the quenching of the nuclear activities. This is not likely to be the case for the stochastic increasing of  $M_{*,\text{sph}}$  due to minor mergers or other dynamical processes like disk instabilities.

In addition, we note that estimation of the intrinsic scatter of the  $M_{\bullet} - M_{*,\text{sph}}$  (or  $M_{\bullet} - \sigma$ ) relation needs to determine the measurement errors in both the MBH and stellar masses, and it is still challenging to accurately determine these measurement errors (see discussions in Graham et al. 2011). Graham (2012) shows that the total scatter could range from 0.44 dex to 0.7 dex for different types of galaxies (see Table 1 therein).

#### 4.3. Alternative $M_{\bullet} - M_{*,\text{sph}}$ or $M_{\bullet} - \sigma$ relation

In the analysis in Section 3, we adopt the single power-law form for the  $M_{\bullet} - M_{*,\text{sph}}$  relation given by Häring & Rix (2004). Recently Graham (2012) suggests that this relation may be better described by a broken power-law than the single power-law shown in Equation (1). To see the effects of this new development on the constraints obtained above, here we replace the  $M_{\bullet} - M_{*,\text{sph}}$  relation at  $z = 0$  shown in Equation (1) by the broken power-law form given in Graham (2012), i.e.,  $\langle \log M_{\bullet} \rangle (M_{*,\text{sph}}; z = 0) = (8.38 \pm 0.17) + (1.92 \pm 0.38) \log[M_{*,\text{sph}} / (7 \times 10^{10} M_{\odot})]$  at  $M_{*,\text{sph}} < 7 \times 10^{10} M_{\odot}$  and  $(8.40 \pm 0.37) + (1.01 \pm 0.52) \log[M_{*,\text{sph}} / (7 \times 10^{10} M_{\odot})]$  at  $M_{*,\text{sph}} \geq 7 \times 10^{10} M_{\odot}$ , respectively. Similarly, we also assume that the intrinsic scatter of this relation is 0.3 dex. By doing the same analysis as that in Section 3, we obtain the constraints on  $(\Gamma, \epsilon)$  as  $(0.44_{-0.75}^{+0.74}, 0.06_{-0.01}^{+0.04})$ . The best fit value of  $\Gamma = 0.44$  is still consistent with that obtained in Section 3  $(0.64_{-0.29}^{+0.27})$  within  $1 - \sigma$  error but its uncertainty  $(_{-0.75}^{+0.74})$  is large. Compared with the constraints on  $(\Gamma, \epsilon)$  obtained for the

single power-law  $M_{\bullet} - M_{*,\text{sph}}$  relation, the larger uncertainty of  $\Gamma$  obtained here is mainly because the relative larger uncertainties in the slope of the broken power-law  $M_{\bullet} - M_{*,\text{sph}}$  relation adopted here lead to larger uncertainties in the estimations of the MBH mass densities compared with that for the single power-law  $M_{\bullet} - M_{*,\text{sph}}$  relation adopted above. The  $\epsilon$  obtained here (0.06) is also substantially smaller than that obtained for the single power-law  $M_{\bullet} - M_{*,\text{sph}}$  relation, mainly because of the relatively higher zero-point of the broken power-law given by Graham (2012).

In the analysis in Section 3, we also adopt the single power-law form for the  $M_{\bullet} - \sigma$  relation given by Gültekin et al. (2009), which is largely consistent with those estimated by others (see references therein). Recently, Graham et al. (2011) updated the  $M_{\bullet} - \sigma$  relation and found that this relation for the barred galaxies may be different from that for those non-barred galaxies/ellipticals. If assuming that the  $M_{\bullet} - \sigma$  relation is the same as that for ellipticals at  $\sigma > 180 \text{ km s}^{-1}$  [i.e.,  $\langle \log M_{\bullet} \rangle (\sigma; z = 0) = (8.22 \pm 0.09) \pm (5.30 \pm 0.77) \log(\sigma / 200 \text{ km s}^{-1})$  with an intrinsic scatter of 0.29] and the same as that for the barred galaxies at  $\sigma < 180 \text{ km s}^{-1}$  [i.e.,  $\langle \log M_{\bullet} \rangle (\sigma; z = 0) = (8.15 \pm 0.06) \pm (5.95 \pm 0.44) \log(\sigma / 200 \text{ km s}^{-1})$  with an intrinsic scatter of 0.35; see Table 2 in Graham et al. 2011], we find  $(\Gamma, \epsilon) = (-0.86_{-0.30}^{+0.31}, 0.14_{-0.01}^{+0.02})$ . The constraint obtained here for  $\Gamma$  is substantially different from that obtained in Section 3, which suggests a significant negative evolution of the velocity dispersion of individual big galaxies, i.e., the velocity dispersions of big galaxies decrease by  $\sim 20\%$ , which is marginally compatible with the hierarchical galaxy formation scenario as recently proposed by Oser et al. (e.g., 2010, 2012). However, the  $\epsilon$  obtained here is slightly higher than that obtained above for a single power-law  $M_{\bullet} - \sigma$  relation, which is mainly due to the smaller intrinsic scatter of the adopted  $M_{\bullet} - \sigma$  relation and the smaller normalization for the relation at  $\sigma < 180 \text{ km s}^{-1}$ . Both of those factors lead to slightly smaller MBH mass densities in all the redshift bins and hence slightly higher  $\epsilon$ .

## 5. CONCLUSIONS

In this paper, we study the cosmic evolution of the  $M_{\bullet} - M_{*,\text{sph}}$  relation and the  $M_{\bullet} - \sigma$  relation by a global method, independent of individual MBH mass estimates. We have estimated the cosmic evolution of MBH mass densities over the redshift range of  $z \sim 0 - 1.2$ . The MBH mass densities are estimated from both the SMFs/VDFs of normal galaxies determined by recent observations using the  $M_{\bullet} - M_{*,\text{sph}}$  and  $M_{\bullet} - \sigma$  relations, and the AGN X-ray LFs according to the simple Sołtan (1982) argument. By matching the MBH densities estimated from the normal galaxies with that from the AGN X-ray LFs, we obtain global constraints on the evolution of the  $M_{\bullet} - M_{*,\text{sph}}$  relation and the  $M_{\bullet} - \sigma$  relation. We find that the  $M_{\bullet} - M_{*,\text{sph}}$  relation evolves with redshift positively, i.e.,  $\propto (1+z)^{\Gamma}$  and  $\Gamma = 0.64_{-0.29}^{+0.27}$ , though the significance level is not high; however, a  $\Gamma$  larger than 1.6 is excluded at the  $3\sigma$  level. We also find that the  $M_{\bullet} - \sigma$  relation appears not to positively evolve with redshift ( $\Gamma = -0.21_{-0.33}^{+0.28}$ ). Our results suggest that the MBH mass growth precedes the bulge mass growth but

the galaxy velocity dispersion does not increase with the mass growth of the bulge after the quench of nuclear activity, which is roughly consistent with the two-phase galaxy formation scenario proposed by Oser et al. (2012) in which a galaxy roughly double its masses after  $z = 1$  due to accretion and minor mergers while its velocity

dispersion drops slightly.

We thank the referee for helpful comments. This work was supported in part by the National Natural Science Foundation of China under nos. 10973001, 10973017, 11033001, and by the Bairen program from the National Astronomical Observatories, Chinese Academy of Sciences.

#### REFERENCES

- Aird, J., et al. 2010, *MNRAS*, 401, 2531  
 Alexander, D. M., et al. 2008, *AJ*, 135, 1968  
 Bell E. F., & de Jong R. S. 2001, *ApJ*, 550, 212  
 Bell, E. F., McIntosh, D. H., Katz, N., & Weinberg, M. D. 2003, *ApJS*, 149, 289  
 Bennert, V. N., Auger, M. W., Treu, T., Woo, J.-H., & Malkan, M. A. 2011, *ApJ*, 742, 107  
 Bennert, V. N., Treu, T., Woo, J.-H., Malkan, M. A., Le Bris, A., Auger, M. W., Gallagher, S., & Blandford, R. D. 2010, *ApJ*, 708, 1507  
 Bernardi, M., Shankar, F., Hyde, J. B., Mei, S., Marulli, F., & Sheth, R. K. 2010, *MNRAS*, 404, 2087  
 Bezanson, R., et al. 2011, *ApJ*, 737, L31  
 Borch, A., et al. 2006, *A&A*, 453, 869  
 Bower, R. G., Benson, A. J., Malbon, R., Helly, J. C., Frenk, C. S., Baugh, C. M., Cole, S., & Lacey, C. G. 2006, *MNRAS*, 370, 645  
 Chabrier, G. 2003, *ApJ*, 586, L133  
 Cisternas, M., Jahnke, K., Bongiorno, A., Inskip, K. J., Impey, C. D., Koekemoer, A. M., Merloni, A., Salvato, M., & Trump, J. R. 2011, *ApJ*, 741, L11  
 Collin, S., Kawaguchi, T., Peterson, B. M., & Vestergaard, M. 2006, *A&A*, 456, 75  
 Croton, D. J., Springel, V., White, S. D. M., De Lucia, G., Frenk, C. S., Gao, L., Jenkins, A., Kauffmann, G., Navarro, J. F., & Yoshida, N. 2006, *MNRAS*, 365, 11  
 Davis, S. W., & Laor, A. 2011, *ApJ*, 728, 98  
 Di Matteo, T., Springel, V., & Hernquist, L. 2005, *Nature*, 433, 604  
 Ebrero, J., et al. 2009, *A&A*, 493, 55  
 Fabian, A. C. 1999, *MNRAS*, 308, L39  
 Ferrarese, L., & Merritt, D. 2000, *ApJ*, 539, L9  
 Fontana, A., et al. 2006, *A&A*, 459, 745  
 Fontanot, F., Monaco, P., Cristiani, S., & Tozzi, P. 2006, *MNRAS*, 373, 1173  
 Fukugita, M., Shimasaku, K., Ichikawa, T. 1995, *PASP*, 107, 945  
 Gebhardt, K., et al. 2000, *ApJ*, 539, L13  
 Graham, A. W. 2012, *ApJ*, 746, 113  
 Graham, A. W., & Driver, S. P. 2007, *MNRAS*, 380, L15  
 Graham, A. W., & Worley, C. C. 2008, *ApJ*, 388, 1708  
 Graham, A. W., Onken, C. A., Athanassoula, E., & Combes, F. 2011, *MNRAS*, 412, 2211  
 Granato, G. L., De Zotti, G., Silva, L., Bressan, A., & Danese, L. 2004, *ApJ*, 600, 580  
 Gültekin, K., et al. 2009, *ApJ*, 698, 198  
 Häring, N., & Rix, H.-W. 2004, *ApJ*, 604, L89  
 Hawley, J. F., Beckwith, K., & Krolik, J. H. 2007, *Ap&SS*, 311, 117  
 Hopkins, P. F., Richards, G. T., & Hernquist, L. 2007, *ApJ*, 654, 731  
 Ilbert, O., et al. 2010, *ApJ*, 709, 644  
 Jahnke, K., et al. 2009, *ApJ*, 706, L215  
 King, A. 2003, *ApJ*, 596, L27  
 Kisaka, S., & Kojima, Y. 2010, *MNRAS*, 405, 1285  
 Kollatschny, W., & Zetzl, M. 2011, *Nature*, 470, 366  
 Komatsu, E., Dunkley, J., Nolta, M. R., et al. 2009, *ApJS*, 180, 330  
 Kormendy, J., & Richstone, D. 1995, *ARA&A*, 33, 581  
 Krolik, J. H. 2001, *ApJ*, 551, 72  
 La Franca, F., et al. 2005, *ApJ*, 635, 864  
 Lamastra, A., Menci, N., Maiolino, R., Fiore, F., & Merloni, A. 2010, *MNRAS*, 405, 29  
 Li, G., Conroy, C., & Loeb, A. 2012, arXiv:1110.0017  
 Li, Y. R., Wang, J. M., & Ho, L. C. 2012, *ApJ*, 749, 187  
 Magorrian, J., et al. 1998, *AJ*, 115, 2285  
 Maio, U., Dottì, M., Petkova, M., Perego, A., & Volonteri, M. 2012, arXiv:1203.1877  
 Malbon, R. K., Baugh, C. M., Frenk, C. S., & Lacey, C. G. 2007, *MNRAS*, 382, 1394  
 Malizia, A., Stephen, J. B., Bassani, L., Bird, A. J., Panessa, F., & Ubertini, P. 2009, *MNRAS*, 399, 944  
 Marconi, A., et al. 2004, *MNRAS*, 351, 169  
 Marconi, A., & Hunt, L. K. 2003, *ApJ*, 589, L21  
 Martínez-Sansigre, A., & Rawlings, S. 2011, *MNRAS*, 414, 1937  
 McLure, R. J., & Dunlop, J. S. 2001, *MNRAS*, 327, 199  
 McLure, R. J., & Dunlop, J. S. 2002, *MNRAS*, 331, 795  
 Merloni, A., et al. 2010, *ApJ*, 708, 137  
 Murray, N., Quataert, E., & Thompson, T. A. 2005, *ApJ*, 618, 569  
 Netzer, H., & Marziani, P. 2010, *ApJ*, 724, 318  
 Onken, C. A., Ferrarese, L., Merrit, D., Peterson, B. M., Pogge, R. W., Vestergaard, M., & Wandel, A. 2004, *ApJ*, 615, 645  
 Oser, L., Naab, T., Ostriker, J. P., & Johansson, P. H. 2012, *ApJ*, 744, 63  
 Oser, L., Ostriker, J. P., Naab, T., Johansson, P. H., & Burkert, A. 2010, *ApJ*, 725, 2312  
 Peng, C. Y., Impey, C. D., Rix, H. W., Kochanek, C. S., Keeton, C. R., Falco, E. E., Lehár, J., & McLeod, B. A. 2006, *ApJ*, 649, 616  
 Pérez-González P. G. et al. 2008, *ApJ*, 675, 234  
 Portinari, L., Kotilainen, J., Falomo, R., & Decarli, R. 2012, *MNRAS*, 420, 732  
 Raimundo, S. I., Fabian, A. C., Vasudevan, R. V., Gandhi, P., & Wu, J. 2012, *MNRAS*, 419, 2259  
 Robertson, B., Hernquist, L., Cox, T. J., Di Matteo, T., Hopkins, P. F., Martini, P., & Springel, V. 2006, *ApJ*, 641, 90  
 Salucci, P., Szuszkiewicz, E., Monaco, P., & Danese, L. 1999, *MNRAS*, 307, 637  
 Salviander, S., Shields, G. A., Gebhardt, K., & Bonning, E. W. 2007, *ApJ*, 662, 131  
 Sarria, J. E., et al. 2010, *A&A*, 522, L3  
 Schulze, A., & Wisotzki, L. 2011, *A&A*, 535, 87  
 Shankar, F., Salucci, P., Granato, G. L., De Zotti, G., & Danese, L. 2004, *MNRAS*, 354, 1020  
 Shankar, F., Weinberg, D. H., & Miralda-Escidé, J. 2009, *ApJ*, 690, 20  
 Shapiro, S. L. 2005, *ApJ*, 620, 59  
 Shen, J., Vanden, B., Daniel, E., Schneider, D. P., & Hall, P. B. 2008, *AJ*, 135, 928  
 Shields, G. A., Gebhardt, K., Salviander, S., Wills, B. J., Xie, B., Brotherton, M. S., Yuan, J., Dietrich, M. 2003, *ApJ*, 583, 124  
 Silk, J., & Rees, M. J. 1998, *A&A*, 331, L1  
 Silverman, J. D., et al. 2008, *ApJ*, 679, 118  
 Sołtan, A. 1982, *MNRAS*, 200, 115  
 Somerville, R. S. 2009, *MNRAS*, 399, 1988  
 Somerville, R. S., Hopkins, P. F., Cox, T. J., Robertson, B. E., & Hernquist, L. 2008, *MNRAS*, 391, 481  
 Springel, V., et al. 2005, *Nature*, 435, 629  
 Thorne, K. S. 1974, *ApJ*, 191, 507  
 Tremaine, S., et al. 2002, *ApJ*, 574, 740  
 Treu, T., Woo, J.-H., Malkan, M. A., & Blandford, R. D. 2007, *ApJ*, 667, 117  
 Ueda, Y., Akiyama, M., Ohta, K., & Miyaji, T. 2003, *ApJ*, 598, 886  
 Vasudevan, R. V., & Fabian, A. C. 2007, *MNRAS*, 381, 1235  
 Volonteri, M., Madau, P., Quataert, E., & Rees, M. J. 2005, *ApJ*, 620, 69

- Weinzirl, T., Jogee, S., Khochfar, S., Burkert, A., & Kormendy, J. 2009, *ApJ*, 696, 411
- Woo, J.-H., Treu, T., Malkan, M. A., & Blandford, R. D. 2006, *ApJ*, 645, 900
- Woo, J.-H., Treu, T., Malkan, M. A., & Blandford, R. D. 2008, *ApJ*, 681, 925
- Wyithe, J. S. B., & Loeb, A. 2003, *ApJ*, 595, 614
- Yenko, B., Barger, A. J., Trouille, L., & Winter, L. M. 2009, *ApJ*, 698, 380
- Yu, Q., & Lu, Y. 2004, *ApJ*, 602, 603
- Yu, Q., & Lu, Y. 2008, *ApJ*, 689, 732
- Yu, Q., & Tremaine, S. 2002, *MNRAS*, 335, 965
- Zucca, E., et al. 2006, *A&A*, 455, 879